

5

Early Differentiation and Core Formation: Processes and Timescales

Francis Nimmo¹ and Thorsten Kleine²

ABSTRACT

The Earth's core formed via a series of high-energy collisions with already-differentiated objects, likely resulting in several distinct magma ocean epochs. The cores of these impactors probably underwent only limited emulsification and moderate (~50%) isotopic re-equilibration with the target mantle during the collision. Later impactors likely originated from more distant regions of the inner Solar System and were plausibly more volatile-rich and more oxidized than earlier impactors. Short-lived isotopes, especially the hafnium-tungsten (Hf-W) system, provide the strongest constraints on the timescale of accretion and core formation. These short-lived isotopes and dynamical models provide a mutually self-consistent, albeit approximate, chronology. Terrestrial core formation took more than 30 Myr but less than about 200 Myr to complete.

5.1. INTRODUCTION

The Earth—and the other terrestrial planets—are differentiated bodies, a metallic core overlain by a silicate mantle. But the nebula from which these planets ultimately formed originally consisted mainly of undifferentiated dust grains. The aim of this chapter is to review how and when the process of differentiation is thought to have taken place.

In the first half of this chapter we focus on “how”; how did the planets ultimately grow, and by what mechanisms

did core formation take place? In the second half, we focus on “when”; what evidence do we have for the timescales of melting and core formation? Although the main focus of this chapter is the Earth, the processes of accretion and differentiation are general. As a result, considerable insight can be gained by looking at the evidence from both meteorites and other terrestrial bodies, and we do so briefly in this chapter.

The contents of this chapter are closely related to others in this volume. In particular, the processes by which the elemental and stable isotopic composition of the core were established are examined in Chapter 6. We do not focus on silicate differentiation (mantle melting and crust formation), which is treated in more detail in Chapter 8. Nor do we discuss the final addition of material to the mantle (the “late veneer”) after core formation effectively ceased (see Chapter 4).

¹*Department Earth and Planetary Sciences, University of California, Santa Cruz, California, USA*

²*Institut für Planetologie, Westfälische Wilhelms-Universität Münster, Münster, Germany*

This chapter covers similar ground to various earlier reviews. An old but still useful treatment of the physics of core formation is given by *Stevenson* [1990]; an accessible survey of the earliest Earth is by *Zahnle et al.* [2007]. A comprehensive review with a similar scope to this one may be found in *Rubie et al.* [2015].

5.1.1. How Does Core Formation Occur?

In one sense, core formation is a very simple process. It is energetically favorable for the densest components of a planet (the metals) to sink to the center. However, this redistribution of mass requires deformation of some kind to occur. Neither metals nor silicates are particularly deformable at low temperatures, and as a result, core formation can only occur at elevated temperatures (Section 5.1.1.3). As we discuss in Section 5.1.1.2, the extent to which planetary bodies are heated as they grow depends on the details of the accretion process. Our current understanding of terrestrial planet accretion is summarized in Section 5.1.1.1.

An important conclusion, at least for the Earth, is that many of the bodies that formed the Earth were themselves already differentiated. As a result, the idea of there being a single instant of core formation is too simple; in reality, the delivery of a metallic component to the deep interior happened many times, and potentially by several different mechanisms. To the extent that it implies a single event, “core formation” is thus a misnomer. We nonetheless continue to employ it as useful shorthand for the processes by which metallic materials are transported to depth.

5.1.1.1. Overview of Accretion in the Terrestrial Planet Zone

The processes of planetary accretion and core growth are inextricably linked. Planets grow via collisions, which both deliver core material and produce conditions under which differentiation is favored (see below). As a result, we will begin with a brief overview of accretion. More detailed reviews may be found in *Chambers* [2010], *Morbidelli et al.* [2012], and Chapter 3.

Conventionally, terrestrial planet accretion is thought to occur in four stages. The initial growth from micron-sized dust grains to kilometer-sized bodies is not well understood, because of the tendency of meter-scale bodies to break themselves apart. Nonetheless, this process must have occurred rapidly—in perhaps 10^3 years—to avoid loss of the dust grains via gas drag. Kilometer-scale bodies are large enough to start perturbing their neighbors’ orbits, at which point a second stage, that of runaway growth, ensues. In this stage, larger bodies are more effective in focusing impacts than their smaller neighbors, and so grow more rapidly, becoming yet more effective and so

on. This process slows once the local feeding zone is exhausted, and transitions into the more orderly third stage of oligarchic growth [*Kokubo and Ida*, 1998]. At a few Myr after Solar System formation, the region around 1AU will have contained tens of Moon- to Mars-sized “embryos” embedded within a cloud of surviving smaller planetesimals. At about the same time, early stellar activity will have removed any remaining gas and dust not already incorporated into larger objects. The presence of gas is important because it can drive planetary migration. For instance, early migration of Jupiter and Saturn may have sculpted the protoplanetary disk from which the terrestrial planets subsequently formed, potentially explaining the small mass of Mars [*Walsh et al.*, 2011].

The final stage of terrestrial planet accretion involves growth via collisions with embryos; typical timescales for this process are tens of Myr [e.g., *Agnor et al.*, 1999]. From the point of view of the early Earth, this stage is the most important, because it involves the largest transfers of mass and energy (see below). Because of the relatively small number of bodies involved, this process can be modeled relatively easily. Unfortunately, however, the process is stochastic, and so there are many different growth scenarios that could have yielded the early Earth.

Figure 5.1 shows the typical growth history of an Earth-like body (bold line), from the numerical simulations of *Raymond et al.* [2006]. Growth occurs mainly via half-a-dozen or so collisions with comparable-sized objects; although there is a steady background mass accumulation via small impacts, the total mass fraction contributed by this process is small. This kind of growth history can be crudely approximated by continuous growth at an exponentially-decreasing rate (thin line). Although this kind of analytical model is advantageous for modeling the isotopic effects of core formation (see Section 5.2.3 below), it does not capture the discontinuous, stochastic nature of the real accretion process.

Beyond the discontinuous, stochastic nature of Earth’s growth, there are two other relevant characteristics of accretion. First, the “feeding zone” from which the proto-Earth accretes material expands with time [*O’Brien et al.*, 2006, 2014; *Bond et al.*, 2010]. As a result, material delivered later in the accretion process tends to have originated at greater distances from the Sun. This result is potentially important for volatile content and partitioning behavior of siderophile elements during core formation (see Section 5.2.3.3). Second, in reality only roughly one in every two collisions actually result in the two bodies merging [*Kokubo and Genda*, 2010, *Chambers*, 2013]; other collisions are either “hit-and-run” events [*Asphaug et al.*, 2006] or (more rarely) result in net mass loss (erosion) of the target body. Hit-and-run events prolong the duration of the final stages of accretion. Erosive events are important because they can change the bulk composition

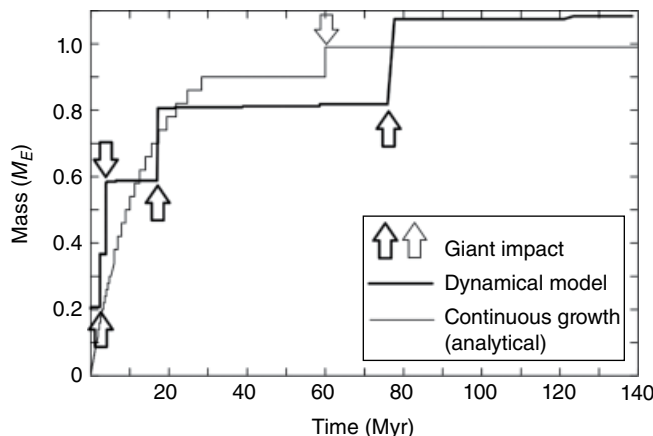


Figure 5.1 Bold line shows a typical growth curve from an N-body simulation [run2a of *Raymond et al.*, 2006]; arrows indicate giant impacts. The thin line assumes growth at an exponentially decaying rate (equation 5.4) with a timescale τ of 10 Myr and a later final Moon-forming impact. Exponential growth models with longer e-folding time-scales have been used to reproduce the Hf-W and U-Pb isotope systematics of the Earth [*Halliday*, 2004; *Rudge et al.*, 2010] under the assumption of incomplete re-equilibration during impacts (Section 5.2.4.1). M_E is one Earth mass.

(and isotopic signature) of the target bodies [*Dwyer et al.*, 2015]; for instance, the Earth may have a non-chondritic bulk composition (see Chapter 2) thanks to preferential impact removal of incompatible elements contained in the crust [*O'Neill and Palme*, 2008]. We discuss this issue further below.

5.1.1.2. Thermal State of Accreting Bodies

Since core formation requires elevated temperatures, we need to consider possible heat sources available during accretion. There are two principal sources. The first is the decay of short-lived radioisotopes, the most important of which is ^{26}Al with a half-life of ~ 0.7 Myr; ^{60}Fe with a half-life of ~ 2.6 Myr was probably not present in sufficient quantities to be important [*Tang and Dauphas*, 2012]. The heat conduction timescale for a silicate sphere of radius R is given by $R^2/\pi^2\kappa$ where κ is the thermal diffusivity; the resulting timescale is ~ 0.7 Myr $(R/15 \text{ km})^2$. Consequently, an asteroid that grows to a diameter much greater than 30 km within the first Myr or so will be unable to conduct away the heat produced by ^{26}Al and will thus experience heating. The exact amount of heating will depend on the details of the growth process, but ^{26}Al is enormously energetic. The total energy released by ^{26}Al decay is sufficient to heat typical chondritic materials by about 4000 K [*Rubie et al.*, 2015]. As a result, early-formed bodies will certainly experience widespread melting (and there is now abundant evidence that this actually happened as discussed below).

The second energy source is the release of gravitational energy. Crudely speaking, an impactor's kinetic energy is (largely) converted into heating the target, with the depth to which this heat is buried depending on the impactor size. As long as the impactors are not too small, the heat

will be buried sufficiently deep that cooling via radiation is ineffective, and as a result the body heats up. In the simplest scenario, this effect results in an inverted temperature profile (later impactors deliver more energy), but for Earth-sized bodies, this effect is likely to be overwhelmed by the deep, heterogeneous heating and mixing caused by giant impacts.

Assuming all the gravitational energy is converted to heat, the globally-averaged temperature increase ΔT due to accretion of a planet of mass M is given by $\Delta T = 3GM/5RC_p \approx 35,000 \text{ K} (M/M_E)^{2/3}$, where M_E is the mass of the Earth and C_p is the specific heat capacity [e.g., *Rubie et al.*, 2015]. This highly simplified calculation neglects the likely large lateral and radial variations in temperature due to giant impacts [e.g., *Canup*, 2004] and the subsequent redistribution of material via rebound and relaxation [*Tonks and Melosh*, 1993]. Nonetheless, it serves to illustrate that Earth- and Mars-sized ($M=0.1 M_E$) bodies are likely to have undergone extensive melting, whereas for an object the size of Vesta ($M=5 \times 10^{-5} M_E$) gravitational heating is insignificant.

An additional source of heat is further gravitational potential energy release as iron sinks toward the center of the planet [*Stevenson*, 1990]. This heat-source is small compared to the total impact energy but can serve to accelerate the iron transport process because the heat is deposited locally, reducing local viscosities [e.g., *Ricard et al.*, 2009; *Sramek et al.*, 2010].

5.1.1.2.1. Terrestrial Magma Oceans

It seems inescapable that much of the Earth's mantle was molten during late-stage accretion. However, the depth and duration of these melting episodes are less clear. Impacts tend to deposit less heat at depth than in

the near-surface, while the mantle melting temperature increases quite steeply with depth (~ 1 K/km) [e.g., *Rubie et al.*, 2015]. As a result, it is possible that the lowermost mantle never experienced complete melting. A more detailed discussion of mantle melting and re-freezing may be found in chapters 7 and 8.

The melting history of the mantle depends very strongly on magma ocean lifetimes. If the magma ocean lifetime is long compared to the interval between giant impacts (~ 10 Myr) then complete mantle melting is more likely than if each magma ocean freezes before the next impact. Unfortunately, magma ocean lifetimes are not well understood. Radiative cooling of an exposed convecting magma ocean is rapid (~ 1 kyr) [*Solomatov*, 2000]. On the other hand, if a surface conductive lid develops, or a thick atmosphere is present [*Abe and Matsui*, 1986; *Zahnle et al.*, 2007], cooling timescales can be ~ 100 Myr, which is a big difference. Tidal dissipation could also have extended the lifetime of a partially-molten layer [*Zahnle et al.*, 2007]. Unlike the Moon, where a buoyant Al-rich plagioclase crust developed, any conductive lid on the Earth would be dense (because Al partitions into garnet at higher pressures). Such a lid would have a tendency to founder and/or be disrupted by impacts, both of which would negate its insulating properties. As a result, in the absence of an atmosphere, relatively rapid magma ocean cooling appears likely. This being the case, the Earth probably experienced several magma ocean epochs, with relatively rapid re-freezing following each giant impact event. The apparently high mantle $^3\text{He}/^{22}\text{Ne}$ ratio has been attributed to fractionation as the result of multiple magma ocean episodes [*Tucker and Mukhopadhyay*, 2014].

5.1.1.3. Core Formation Mechanisms

Core formation involves several distinct mechanisms by which a dense metallic phase may be transported to the deep interior: percolation, diking, diapirism, and direct delivery via impacts. More thorough treatments are given in *Stevenson* [1990] and *Rubie et al.* [2015].

The mechanism involving the lowest levels of stress is percolation. Because Fe (and even more so Fe-S) melts at lower temperatures than silicates, undifferentiated small bodies heated internally will tend to develop metallic melts dispersed within a solid silicate matrix. The metal-silicate density contrast will cause the metal to percolate downward. The characteristic timescale for the two phases to separate is the so-called compaction timescale, originally derived for silicate melt percolation [*McKenzie*, 1984]. Because of the high density and low viscosity of molten iron, core formation by percolation is expected to be rapid [*McCoy et al.*, 2006]. However, at least in the absence of shear stresses [*Yoshino et al.*, 2003], percolation requires an interconnected melt network to exist. This in

turn requires either the so-called dihedral angle between melt and solid to be $< 60^\circ$ or the melt fraction to exceed a critical value (typically a few percent). The dihedral angle is likely $> 60^\circ$ in the upper mantle; for the lower mantle it is not yet clear what the dihedral angle is [*Terasaki et al.*, 2007; *Shih et al.*, 2013]. In any event, if percolation were the dominant mechanism in the upper mantle, one would expect to see a few percent metallic iron stranded there, which is not observed.

Percolation involves distributed flow through a solid matrix. However, if sufficiently large bodies of liquid metal develop, the associated stresses may become large enough to permit other transport mechanisms to operate. Although percolation in theory could be important in the lower mantle, the likely accumulation of large iron bodies (e.g., at the base of a magma ocean) implies that other transport mechanisms will dominate. As argued above, iron transport in the upper mantle also takes place by other mechanisms (e.g., sinking through a magma ocean). Lastly, percolation *sensu stricto* is unlikely to operate over an extended depth range, as it requires that the temperature remain above the metallic solidus but below the silicate solidus. In short, percolation is not expected to be an important iron transport mechanism for the proto-Earth.

If the silicates are relatively cold and brittle, transport may occur via fluid-filled cracks, analogous to dikes [*Stevenson*, 1990]. As long as the stresses are sufficient to overcome the fracture toughness of the surrounding material, the rate-limiting process is fluid drag on the crack walls, and as a result downward delivery of iron by this mechanism is very rapid.

Alternatively, if the silicates are warmer they will deform by viscous creep rather than brittle failure. In this case a dense body of iron will act like a diapir, sinking through the deformable silicates. The rate of sinking depends strongly on the size of the diapir and the viscosity of the surrounding material, but it can be rapid (\sim kyrs) [*Ricard et al.*, 2009]. The deformation of this material can lead to heating, which enhances the rate at which the diapir sinks [*Ricard et al.*, 2009; *Sramek et al.*, 2010; *Samuel et al.*, 2010]. This picture is relevant to small impactor cores, which will be decelerated effectively by the mantle and subsequently exhibit laminar flow. It is not relevant to the largest impactors, which will transit the mantle without slowing appreciably (see below).

The above mechanisms all assume an initially solid (or mostly solid) background matrix. However, temperatures may become sufficiently elevated that the silicates also melt (Section 5.1.1.2). In this case, any pre-existing metal will sink at a rate controlled by the viscosity of the molten silicates, which is comparable to that of water [*Rubie et al.*, 2003]. As a result, this sinking process is very rapid, despite the potentially vigorous convection taking place in the molten mantle. One can thus envisage situations in

which a pile-up of metal occurs at the base of a local melt pool (for small impacts) or a global magma ocean. Subsequent deeper transport then occurs via one of the other mechanisms discussed above.

During the final stages of accretion, metallic material is delivered as pre-existing cores contained within impactors of comparable size to the target, striking the target at many km/s. The stresses involved in these giant impacts are so large that the material strength of the target is irrelevant. The entire mantle behaves effectively like a fluid. As a result, simulations show that the impactor core merges with the target core on the free-fall timescale of roughly an hour [e.g., *Canup*, 2004]. The high speed and low viscosity of iron make this kind of process enormously turbulent, something that cannot be adequately captured by numerical models. This process, which probably is most relevant for defining the geochemical and isotopic signature of core formation, is very different from the laminar models of diapir descent described above. Diapirism may occur after small impacts deliver metal to the base of a magma ocean, but it is not an appropriate description of the giant impacts that likely deliver the bulk of the metal content of the Earth's core.

Because of the difficulty in modeling turbulent flow during impacts, the extent to which the impactor core mixes and equilibrates with the target silicates is very poorly understood. Unfortunately, the extent of equilibration is crucial in determining the extent to which metals partition into the mantle and the isotopic consequences of this partitioning. The mixing process is certainly scale-dependent: impactor cores that are small compared to the mantle thickness probably re-mix effectively, while larger ones do not. This issue is discussed in more detail in Section 5.2.3.1.

5.1.1.4. Composition of the Earth's Core

The composition of the Earth's core is important because it is known (to some extent), and thus provides a constraint on how accretion occurred. For instance, as will be seen, different trajectories in oxygen fugacity make quite different predictions about core composition. The core also has an indirect effect, in that core formation is likely to have removed most siderophile elements from the mantle (see Section 5.2.3.3). This process is central to the Hf-W chronometer discussed below. A recent review of core composition appears in *Rubie et al.* [2015], and only a brief summary is given here.

Although the Earth's core is mainly Fe+Ni, it has long been known that the seismically-determined core density is less than that of a simple Fe-Ni alloy. For the outer core the difference is 6 to 10%, with a somewhat smaller difference for the inner core [e.g., *Alfe et al.*, 2002]. Thus, the core must contain one or more light elements, with

commonly-cited suspects including sulfur, silicon, oxygen, and carbon [e.g., *Poirier*, 1994].

The Earth's dynamo is thought to be at least partly driven by compositional convection due to expulsion of light element(s) from the inner core as it solidifies [e.g., *Nimmo*, 2015]. *Alfe et al.* [2002] used first principles computations to argue that O, but not S or Si, is excluded from crystalline iron, and therefore, that O must make up at least part of the light element budget. They concluded that the outer core contains 10+/-2.5% molar S or Si and 8+/-2.5% molar O, while the inner core contains 8.5+/-2.5% molar S/Si.

Whether or not a particular element partitions into the core depends on the pressure, temperature, and oxygen fugacity conditions at the relevant time [e.g., *Tsuno et al.*, 2013]. Measurement of partitioning behavior at the high P,T conditions associated with core formation is experimentally challenging [e.g., *Siebert et al.*, 2013]; moreover, the oxygen fugacity is likely to have evolved as core formation proceeded [e.g., *Wade and Wood*, 2005; *Rubie et al.*, 2011; *Siebert et al.*, 2013], further complicating analysis. Some calculations favor Si as the dominant light element [*Rubie et al.*, 2011; *Ricolleau et al.*, 2011], while others prefer O [*Siebert et al.*, 2013]; S is less popular because of its high volatility [*McDonough*, 2003]. A comparison of experimental and seismically-derived velocities suggest that core concentrations of O are relatively low [*Huang et al.*, 2011] and that S and/or Si are more important [*Morard et al.*, 2013]. A core possessing at least some Si is also consistent with small differences in stable Si isotopes between Earth's mantle and chondrites [*Georg et al.*, 2007], although this difference may also arise from processes within the solar nebula [*Dauphas et al.*, 2014]. At present, the identity of the light element(s) in the Earth's core remains an open question.

One further trace element of potential importance to the core is potassium, because radioactive decay of this element can help drive a long-lived dynamo and influences the long-term temperature evolution of the core [e.g., *Nimmo*, 2015]. K does not appear to partition efficiently into metal, at least under moderate P,T conditions [*Bouhifd et al.*, 2007; *Corgne et al.*, 2007], and the deficiency of K relative to U and Th in the Earth's mantle compared to chondrites is readily explained by potassium's greater volatility. Ultimately, geoneutrino studies [e.g., *Araki et al.*, 2005] should directly constrain how much (if any) potassium the core contains.

5.1.1.5. Lessons from Other Bodies

So far, we have treated the processes involved in core formation theoretically. Fortunately, however, in most cases there is observational evidence for the processes described. Here we will briefly discuss pertinent observations from bodies other than the Earth. For the Earth, we

summarize the likely processes operating in Section 5.1.1.6 below, and discuss the chronology of core formation in more detail in Section 5.2.

Abundant evidence exists for differentiation and core formation in asteroids. Perhaps most obviously, magmatic iron meteorites and metallic parent bodies (such as 16 Psyche) require core formation to have occurred, while differentiated achondrites are depleted in siderophile elements [e.g., *Mittlefehldt et al.*, 1998], indicating loss of metal due to core formation. The size of the parent bodies in which this differentiation took place is roughly constrained by cooling rates estimated from exsolution textures [e.g., *Yang and Goldstein*, 2006]. Typical diameters are 30–100 km. Some rapid cooling rates have been attributed to bodies in which the silicate mantle was stripped by a giant impact [*Yang et al.*, 2007], in which case the pre-impact body could have been larger. Even in this case, however, gravitational heating would still be insufficient to cause melting (see above). On the other hand, these sizes are sufficient to cause melting due to ^{26}Al decay if the bodies formed early enough. The Hf-W chronometer (see below) suggests that the parent bodies of magmatic iron meteorites formed and differentiated within ~ 2 Myr after formation of the earliest known Solar System solids, calcium-aluminium inclusions, or CAIs [e.g., *Kruijer et al.*, 2014a], and were therefore certainly subject to ^{26}Al heating.

On the other hand, the existence of chondritic meteorites implies that not all asteroids underwent differentiation. Because of the rapid decay of ^{26}Al , bodies that accreted more than 2–3 Myr after Solar System formation are unlikely to have experienced enough heating to undergo differentiation. Chondrites, therefore, either derive from very small bodies or from bodies that accreted more than ~ 2 Myr after CAI formation. A recent suggestion is that some chondrites are samples from the surface of differentiated asteroids [*Elkins-Tanton et al.*, 2011]. In any event, relatively small changes in the rate of growth can have very dramatic effects on the thermal evolution of a body, and thus whether or not it underwent differentiation.

Interestingly, some classes of meteorites appear to have been caught in the act of differentiation. Hand-specimen size samples of acapulcoites and lodranites show evidence for localized formation of metal melts, which, however, did not fully segregate [*McCoy et al.*, 2006]. Hf-W isotope systematics suggest that such bodies accreted 1.5–2 Myr after CAI formation [*Touboul et al.*, 2009], consistent with moderate heating by ^{26}Al decay.

As noted above, gravitational energy alone is probably sufficient to cause differentiation and core formation on Mars. However, the growth of Mars (as measured by the Hf-W isotopic system, Section 5.2.1) may have been sufficiently rapid that ^{26}Al also played a role [*Dauphas and Pourmand*, 2011], although the Hf-W age of core formation

in Mars is debated [*Mezger et al.*, 2013; *Nimmo and Kleine*, 2007]. As noted above, there are dynamical scenarios that permit this kind of rapid growth to occur. From our point of view, Mars is important because it likely represents the kind of precursor body from which the Earth was built. Early core formation in these precursor bodies could have potentially important consequences for the Hf-W isotope systematics of the Earth's mantle (see below).

The Moon probably formed as the result of a giant impact onto the proto-Earth. The small core size and volatile-depleted nature of the Moon is a consequence of this unusual mode of formation. Although many dynamical aspects of this event remain uncertain (such as impactor size, mass fraction of impactor material in the Moon) [*Cuk and Stewart*, 2012; *Canup*, 2012], the isotopic similarities between the Earth and the Moon are most easily accounted for if the Moon is largely derived from the Earth's mantle [*Zhang et al.*, 2012] or if both the Earth and impactor formed at similar heliocentric distances from a homogeneous inner disk reservoir [*Wiechert et al.*, 2001; *Dauphas et al.*, 2014]. The Earth-Moon W isotope similarity is not easily explained in either case, however, because the different mixing proportions of impactor material in the Moon and bulk silicate Earth should lead to W isotope heterogeneities [*Touboul et al.*, 2007; *Kruijer et al.*, 2015], unless very specific impactor and proto-Earth compositions and giant impact conditions are invoked [*Dauphas et al.*, 2014]. The Moon-forming impact is generally assumed to be the last large impact that the Earth experienced, and as such its formation marks the effective end of the main phase of core formation. We discuss this issue further below in Section 5.2.5. The Moon is also relevant because it may provide a record of the Earth's mantle prior to the waning stage of accretion.

5.1.1.6. Summary: Core Formation Processes on Earth

Core formation on Earth was a multi-stage process, with the majority of the metal being delivered to the proto-Earth by giant impacts with already-differentiated bodies. These impacts were highly energetic and resulted in massive melting of significant fractions of the mantle. Although the evidence is not conclusive, it is likely that the resulting magma ocean lifetimes were short compared to the interval between large impacts. These multiple melting episodes likely allowed mantle heterogeneities to develop and persist.

For the largest impacts, the impactor core's passage through the mantle was rapid (\sim hours) and emulsification and mixing was probably restricted; as a result, chemical or isotopic re-equilibration with the silicates will have been limited. Smaller impactor cores may have undergone more complete emulsification, resulting in ponding of metallic material at the base of the magma ocean and subsequent downward transport by diapirism or diking. Figure 5.2 summarizes our physical picture of how core

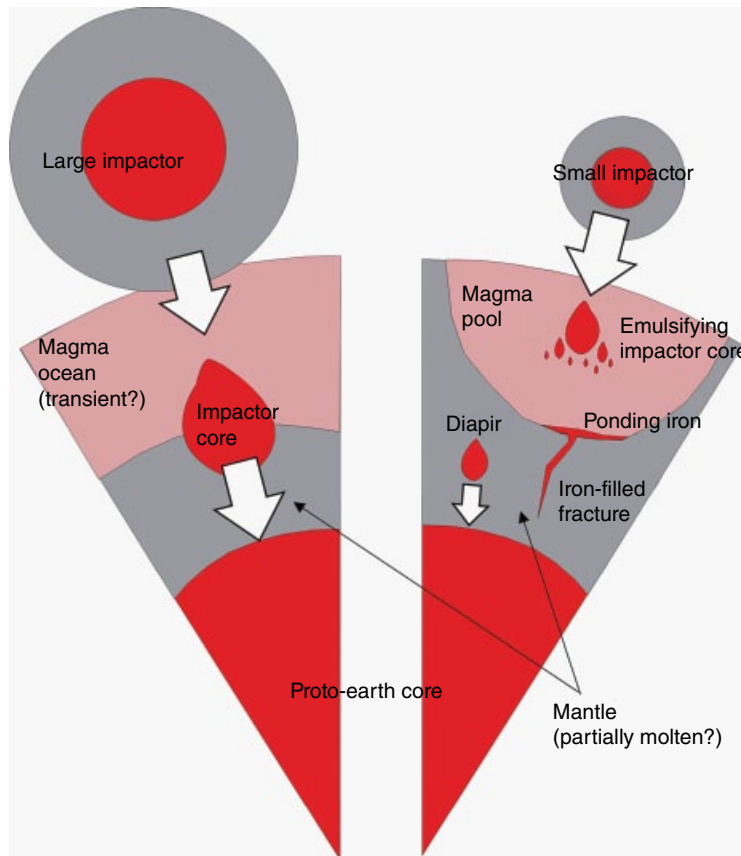


Figure 5.2 Summary picture of the distinct metal segregation mechanisms for large and smaller impacts. Giant impacts probably result in widespread mantle melting and a magma ocean of uncertain but potentially short duration. Such large impacts probably result in minimal emulsification and mixing of the impactor core. If the mantle is initially solid, a small impact will generate a melt pool at the base of which metal will accumulate.

formation proceeds following both large and smaller impacts. In the next section, we discuss the timescales of the relevant processes.

5.2. WHEN DOES IT OCCUR?

There are various unstable isotopes that provide potential chronometers of core formation (and thus accretion). The most useful of these is the hafnium-tungsten (Hf-W) system, which is described in some detail in Sections 5.2.1 to 5.2.3. Other chronometers, principally the palladium-silver (Pd-Ag), uranium-lead (U-Pb), and iodine-xenon (I-Xe) systems, also provide some constraints, and are discussed briefly in Section 5.2.4.

5.2.1. Principles of Hf-W System

A recent and thorough review of the Hf-W system may be found in *Kleine et al.* [2009]. A good overview of theoretical models may be found in *Jacobsen* [2005].

The principles of the system are as follows. The short-lived, now-extinct radionuclide ^{182}Hf decays to ^{182}W with a half-life, $t_{1/2}$, of 8.9 Myr (comparable to the timescale of accretion). Since both Hf and W are refractory, there presumably has been little Hf/W fractionation in the solar nebula, and so the Hf/W ratio of bulk planetary bodies can be assumed to be approximately the same as in chondrites. During core formation, the chondritic Hf/W ratio of an originally undifferentiated body is internally fractionated, because most W will have been removed from the mantle, which will still retain its full complement of Hf. If core formation occurred during the effective lifetime of ^{182}Hf (i.e., ca. 6 half-lives, ~ 50 Myr), then the mantle will develop excess ^{182}W , the magnitude of which depends on the timing of core formation and the Hf/W ratio of the mantle. On the other hand, if core formation occurred after extinction of ^{182}Hf , then no in-growth of mantle ^{182}W will occur. Thus, the amount of excess ^{182}W in the mantle (or the ^{182}W deficit in a core) can be used to establish the timing of core formation. Additional

fractionation may occur during silicate melting, where W is more incompatible than Hf, potentially leading to ^{182}W variations unrelated to core formation (see Section 5.2.2) [Kleine *et al.*, 2004; Foley *et al.*, 2005].

The excess ^{182}W of a sample can be expressed as relative to a CHondritic Uniform Reservoir (CHUR), in which case it is defined as follows:

$$\Delta\varepsilon_W(t) = \left[\frac{\left(\frac{^{182}\text{W}}{^{184}\text{W}} \right)_{\text{sample}}(t)}{\left(\frac{^{182}\text{W}}{^{184}\text{W}} \right)_{\text{CHUR}}(t)} - 1 \right] \times 10^4 \quad (5.1)$$

Note that $\Delta\varepsilon_W(t)$ is time-variable, because $\left(\frac{^{182}\text{W}}{^{184}\text{W}} \right)_{\text{CHUR}}$ varies due to ^{182}Hf decay; also note that for a chondritic material $\Delta\varepsilon_W(t)$ is always zero by definition.

Measured W isotope compositions are usually expressed as ε_W which is the deviation of the present-day $^{182}\text{W}/^{184}\text{W}$ ratio of a sample from that of the terrestrial standard:

$$\varepsilon_W = \left[\frac{\left(\frac{^{182}\text{W}}{^{184}\text{W}} \right)_{\text{sample}}}{\left(\frac{^{182}\text{W}}{^{184}\text{W}} \right)_{\text{standard}}} - 1 \right] \times 10^4 \quad (5.2)$$

Note that for the present-day $\Delta\varepsilon_W = \varepsilon_W + 1.9$, because the present-day ε_W of chondrites is -1.9 [Kleine *et al.*, 2002, 2004; Schönberg *et al.*, 2002; Yin *et al.*, 2002].

Consider an initially chondritic undifferentiated body that undergoes instantaneous core formation at t_{cf} (We will refer to this as a “two-stage” model.) The timing of core formation t_{cf} is given by [e.g., Kleine *et al.*, 2009]

$$t_{\text{cf}} = \frac{1}{\lambda} \cdot \ln \left[\frac{1.59 \cdot f^{\text{Hf/W}}}{\Delta\varepsilon_W} \right] \quad (5.3)$$

Here $f^{\text{Hf/W}}$ is the Hf/W fractionation factor defined as $f^{\text{Hf/W}} = \left[\left(\frac{^{180}\text{Hf}}{^{184}\text{W}} \right)_{\text{sample}} / \left(\frac{^{180}\text{Hf}}{^{184}\text{W}} \right)_{\text{CHUR}} \right] - 1$, where the numerical quantity inside the square brackets in equation (5.3) arises from the difference in present-day $\varepsilon_W = -1.9$ and initial $\varepsilon_W = -3.49$ of chondrites [Burkhardt *et al.*, 2012; Kruijer *et al.*, 2014b] This equation demonstrates that determining a time of core formation requires knowledge of the ^{182}W anomaly and Hf/W ratio characteristic of the entire silicate portion (or the entire metal core) of a differentiated planet. Equation (5.3) also makes clear that for a given Hf/W ratio of the mantle a larger ^{182}W anomaly implies an earlier core formation. It also makes the role of core-mantle partitioning clearer. If tungsten partitions more strongly into the core, then $f^{\text{Hf/W}}$ is larger and the inferred core formation timescale, for a given ^{182}W anomaly, is later.

The two-stage model time (equation 5.3) is useful for assessing the relative speeds of accretion of different

bodies. However, for Earth-sized bodies it should not be taken to represent the actual timing of accretion or core formation, which are both protracted, multi-stage processes. At best, it represents the earliest age at which core formation could have ceased. More realistic core formation models and their consequences for the Hf-W isotope systematics will be discussed in more detail below (see Section 5.2.3).

5.2.2. Hf-W Isotope Systematics of the Earth, Moon, Mars, and Differentiated Asteroids

The Hf-W isotope systematics of differentiated asteroids and terrestrial planets are reasonably well established. The Hf-W data show the expected systematics for core formation during the lifetime of ^{182}Hf . Magmatic iron meteorites as samples of the metallic core of differentiated protoplanets exhibit ^{182}W deficits relative to chondrites, whereas samples derived from the silicate portion of differentiated bodies are characterized by ^{182}W excesses (Fig. 5.3).

Eucrites, angrites, and martian meteorites exhibit variable ^{182}W excesses, which at least in part result from Hf/W fractionation by silicate melting processes during the lifetime of ^{182}Hf [Kleine *et al.*, 2004; Foley *et al.*, 2005; Kleine *et al.*, 2012; Touboul *et al.*, 2015b]. This makes estimating the ε_W of the bulk mantle of these bodies difficult. For Mars there is abundant evidence for early mantle differentiation from variations in $^{142}\text{Nd}/^{144}\text{Nd}$ (from the decay of short-lived ^{146}Sm) [e.g., Debaille *et al.*, 2007]. Some shergottites, however, exhibit near-chondritic $^{142}\text{Nd}/^{144}\text{Nd}$ and can thus be used to estimate the ^{182}W anomaly of the bulk martian mantle prior to mantle differentiation [Kleine *et al.*, 2004; Foley *et al.*, 2005]. This approach leads to $\varepsilon_W = 0.45 \pm 0.15$ for bulk silicate Mars [Kleine *et al.*, 2009]. For the eucrite and angrite parent bodies, the ε_W of the bulk mantle can be determined from the Hf-W isotopic evolution of eucrites and angrites, respectively, which sampled the mantle at different times and, hence, provide a record of the ε_W of the mantle over time. For the angrite parent body at least two mantle reservoirs exist, which probably acquired their distinct Hf/W ratios as a result of metal-silicate fractionation [Kleine *et al.*, 2012]. In this case, there is no single Hf/W and ε_W characteristic of the entire mantle.

Terrestrial and lunar samples show less variable ε_W , but recently small ^{182}W excesses have been reported for Archean samples from Isua, Greenland [Willbold *et al.*, 2011] and the Nuvvuagittuq Greenstone Belt, Quebec, Canada [Touboul *et al.*, 2014], and for some komatiites [Touboul *et al.*, 2012]. These small ^{182}W excesses either reflect the ε_W of the bulk silicate Earth prior to (complete) addition of the late veneer, or result from early differentiation processes within the mantle. Either way, for determining an Hf-W age of core formation in the Earth,

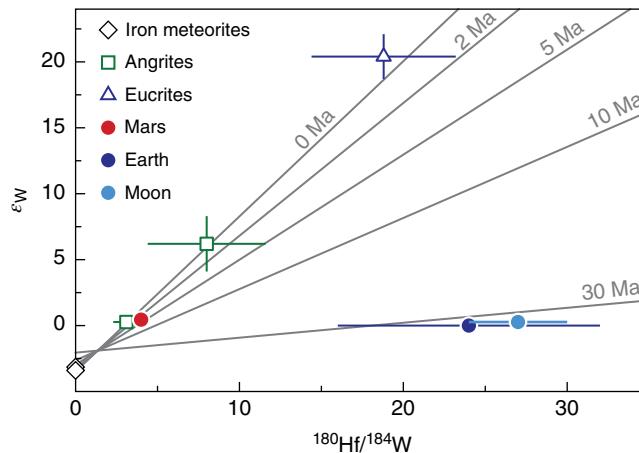


Figure 5.3 Hf-W systematics of differentiated planetary bodies. Data sources as in Table 5.1. Note that chondrites and, hence, undifferentiated bulk planetary objects, plot at $\epsilon_w = -1.9$. Diagonal solid lines indicate different two-stage core formation times (equation 5.3). Longer accretion timescales result in a smaller tungsten anomaly for a given value of $^{180}\text{Hf}/^{184}\text{W}$.

the ϵ_w of the bulk silicate Earth prior to addition of the late veneer should be used. Mass balance indicates that this value should be approximately 0.15–0.40 higher than that of the modern Earth’s mantle, in good agreement with values measured for some Isua samples and komatiites [Willbold *et al.*, 2011; Touboul *et al.*, 2012, 2014]. Lunar samples show variable and large apparent ^{182}W excesses, but these largely result from cosmic ray-induced neutron capture reactions [e.g., Kleine *et al.*, 2009]. Two recent studies have shown that samples unaffected by neutron capture show small but well-resolved ^{182}W excesses of between ~ 0.2 and $\sim 0.3 \epsilon_w$ [Kruijer *et al.*, 2015; Touboul *et al.*, 2015a], in good agreement with the estimated W isotope composition of the pre-late veneer bulk silicate Earth.

Owing to the different incompatibilities of Hf and W during silicate melting, the Hf/W ratio characteristic of the bulk silicate portion of a differentiated planetary body cannot be measured directly. Instead it must be inferred from the ratio of W to a refractory lithophile element of similar incompatibility (such as U and Th) and by assuming chondritic ratios of these refractory lithophile elements relative to Hf (see Table 5.1). Figure 5.3 shows that the bulk silicate portions of the Earth, Moon, and eucrite parent body are characterized by higher Hf/W ratios than those of Mars and the angrite parent body. This highlights the fact that the partitioning of W into metal can vary depending on the conditions of core formation and suggests that core formation in Mars and the angrite parent body occurred under more oxidizing conditions than on the other three bodies (note that the Moon inherited its high Hf/W from the Earth’s mantle).

Table 5.1 summarizes the calculated two-stage model ages (equation 5.3) for core formation in the Earth, Moon,

Mars, and the parent bodies of magmatic iron meteorites. For the eucrite and angrite parent bodies, the two-stage model ages are very imprecise because the ϵ_w and Hf/W of the bulk mantle are poorly constrained. For these bodies, the time of core formation is best determined from the intersection of the Hf-W isotope evolution line of the mantle with the chondritic evolution line [Kleine *et al.*, 2012; Touboul *et al.*, 2015b]. As discussed above, the model timescales of the Earth and Moon and probably also Mars should not be taken literally, because core formation at least in these bodies is not a single event. Nonetheless, it serves to show that the Earth experienced a protracted accretion history, compared to bodies like Mars or the parent bodies of differentiated meteorites, all of which have much shorter two-stage timescales [Kleine *et al.*, 2009].

5.2.3. Multi-stage Core Formation During Accretion of the Earth

As outlined above, assuming instantaneous core formation is not appropriate for Earth-sized bodies, in which core formation was a stochastic, multi-stage process driven by multiple giant impacts. Rather than assuming instantaneous core formation, a better approximation is to model core formation as a continuous process occurring during protracted accretion [e.g., Halliday, 2004; Kleine *et al.*, 2004; Jacobsen, 2005]. This requires an appropriate model for the growth of the Earth and assumptions regarding the degree of re-equilibration of newly accreted material with the mantle of proto-Earth.

To track the isotopic evolution of the Earth, its growth is often assumed to occur at an exponentially decreasing rate (see Fig. 5.1), such that

Table 5.1 Values represent those of the bulk silicate portions or in the case of the iron meteorites of the bulk metal core. For the Earth, ϵ_w has been calculated by subtracting the late veneer (i.e., the pre-late veneer value of the BSE is given) [Kruijer *et al.*, 2015]. Note that for the angrite parent body two mantle reservoirs with distinct $^{180}\text{Hf}/^{184}\text{W}$ and ϵ_w exist [Kleine *et al.*, 2012]. The $^{180}\text{Hf}/^{184}\text{W}$ of the bulk silicate Earth is the average of estimates based on Ta/W [König *et al.*, 2011], Th/W [Newsom *et al.*, 1996; Arevalo and McDonough, 2008], and U/W ratios [Arevalo *et al.*, 2008]. The $^{180}\text{Hf}/^{184}\text{W}$ of the bulk silicate Moon was calculated using Th/W and U/W ratios [Palme and Rammensee, 1981; Münker, 2010], and for both the Earth and Moon chondritic Th/Hf and U/Hf ratios from *Dauphas and Pourmand* [2011] were used. For derivation of ϵ_w values for the Earth and Moon, see the text. $^{180}\text{Hf}/^{184}\text{W}$ for the bulk mantle of Mars is from *Dauphas and Pourmand* [2011], and ϵ_w is from *Kleine et al.* [2009]. Values for eucrites are from *Touboul et al.* [2015b], for angrites from *Kleine et al.* [2012], and for iron meteorites from *Kruijer et al.* [2013, 2014]. $\Delta\epsilon_w$ and $f^{\text{Hf/W}}$ are both relative to chondrites ($\epsilon_w = -1.9$; $^{180}\text{Hf}/^{184}\text{W} = 1.35$). For the Earth, Moon, Mars, and iron meteorites, the two-stage core formation time t_{cf} is calculated from equation 5.3. For eucrites and angrites, the two-stage model age is very uncertain, because the $^{180}\text{Hf}/^{184}\text{W}$ and ϵ_w characteristic for the bulk silicate portion of these bodies is only poorly constrained. For these two bodies the time of core formation is most precisely determined, however, through the intersection of the Hf-W isotope evolution of the mantle with the chondritic evolution line [see *Kleine et al.*, 2012]. Note that the $^{180}\text{Hf}/^{184}\text{W}$ values for the Earth and Moon are slightly different from previously accepted values (which were used in preparing Figures 5.4 and 5.5) due to a recent revision of the chondritic Hf/Th and Hf/U ratios [*Dauphas and Pourmand*, 2011].

	$^{180}\text{Hf}/^{184}\text{W}$	$f^{\text{Hf/W}}$	ϵ_w	$\Delta\epsilon_w$	t_{cf} (Myr)
Earth	24±8	17±6	0.16–0.38	2.06–2.28	~32
Moon	27±3	19±2	0.27±0.04	2.17±0.11	~34
Mars	4.0±0.5	2.0±0.4	0.45±0.15	2.35±0.18	~4
Eucrites	19±4	13±3	21.4±1.7	22.3±1.7	< ~1
Angrites	3.1±0.8	1.3±0.6	0.3±0.5	2.2±0.5	< ~2
	8.0±3.6	4.9±2.7	6.2±2.1	8.1±2.1	< ~2
Iron meteorites	~0	-1	-3.15±0.07	-1.25±0.12	~3.1
			-3.40±0.03	-1.5±0.1	~0.7

$$M(t)/M_E = 1 - e^{-t/\tau} \quad (5.4)$$

where τ is the mean-life of accretion, corresponding to the time to reach 63% of the Earth's mass. Assuming continuous core formation and full metal-silicate equilibration, this model requires a mean-life of accretion of ~11 Myr to generate the observed $\Delta\epsilon_w$ [Yin *et al.*, 2002]. In the specific case of the exponential model, this value of τ corresponds to an end of accretion at ~30 Myr (as given by time to reach 95% of Earth's mass in the exponential model), similar to the two-stage model age [Jacobsen *et al.*, 2005; Rudge *et al.*, 2010]. Note that in case of incomplete equilibration, a longer mean-life of accretion is required to generate the observed $\Delta\epsilon_w$ of the bulk silicate Earth (see below).

5.2.3.1. Re-equilibration During Core Formation in the Earth

In reality, core formation occurred neither as a continuous influx of metallic material, nor as an instantaneous single differentiation event. Instead, it occurred stochastically, when individual impactors (already differentiated) collided with the proto-Earth (Section 5.1.1.1). This being the case, both the pre-history of the impactors and the extent of re-equilibration between metal and silicates during impact are important.

Consider a collision between two differentiated bodies. If there is no re-equilibration between silicates and metal,

then the final ^{182}W anomaly will simply be the mass-weighted average of the two initial anomalies. The earlier isotopic history of the bodies is thus preserved, and the ^{182}W anomaly of Earth's mantle would say nothing about the timescale of core formation within the Earth. On the other hand, if there is complete re-equilibration between the entirety of the Earth's mantle and the metal core of the newly accreted body, the earlier isotopic history of the bodies is erased, and only then would the resulting ^{182}W anomaly entirely reflect core formation in the Earth. Thus, re-equilibration results in the reduction of the ^{182}W excess in the mantle and as such has a very strong effect on the final ^{182}W anomaly observed. Consequently, higher degrees of re-equilibration require faster accretion to generate the same ^{182}W anomaly, and make the final outcome less sensitive to the pre-collision isotopic characteristics of the bodies.

Figure 5.4 shows the effects of incomplete re-equilibration on the calculated growth timescale in the exponential accretion model (equation 5.4). Here k is the fraction of impactor core material re-equilibrated. As can be seen, the inferred time to complete 90% of Earth formation varies strongly, depending on the value of k chosen. High degrees of re-equilibration with rapid growth yield the same isotopic anomaly as lower degrees of re-equilibration and slower growth. Unfortunately, the actual degree of re-equilibration is both poorly understood and probably

time-variable (see below), resulting in significant uncertainty in the actual core formation timescale. Nonetheless, for the Hf-W system, this model suggests that the bulk of Earth formation certainly took more than 30 Myr to complete, and probably was mostly complete within ~ 100 Myr, which is approximately consistent with dynamical models (Figure 5.1; *Jacobson et al.*, 2014). Figure 5.4 also plots similar constraints from the U-Pb system, which are discussed further in Section 5.2.4.1.

Figure 5.4 demonstrates that determining the timescale of accretion and core formation in the Earth requires knowledge of the degree of re-equilibration during impact. Unfortunately, theoretical understanding of the extent of re-equilibration during impacts remains an unsolved problem. Isotopic re-equilibration takes place over lengthscales of ~ 1 cm, based on likely iron transport timescales and diffusivities [*Rubie et al.*, 2003]. Thus, for extensive re-equilibration to occur, the incoming impactor core must be emulsified down to cm-scale droplets, a change in scale of 8 orders of magnitude. Presumably both buoyancy- and shear-instabilities develop at the interface between the

descending impactor and the surrounding (probably molten) mantle [*Dahl and Stevenson*, 2010]. A turbulent cascade develops, reducing the characteristic size of the liquid metal blobs. The key question is therefore how far this process proceeds before the impactor and target core merge.

This kind of question is very hard to answer numerically because of the high degree of turbulence and large range in length-scales involved [*Samuel*, 2012]. Laboratory experiments provide more insight [*Deguen et al.*, 2011; *Deguen*, 2014], and suggest that impactor cores with diameters comparable to the thickness of the magma ocean will not undergo efficient equilibration, while smaller cores will. For a typical body with a (molten) mantle half the radius of the planet, this criterion implies that impactors larger than roughly one-eighth the target mass will not experience efficient equilibration. Such impacts are a common feature of the final stages of accretion (Figure 5.1). Scaling arguments based on turbulent cascades suggest equilibration may be ineffective for impactor cores with radii > 100 km [*Dahl and Stevenson*, 2010]. The effective k , integrated over all impactors, is then only about 0.1. If magma oceans are short-lived features, that again militates against extensive equilibration, because metal transport through a solid mantle tends to require iron bodies with lengthscales $\gg 1$ cm (Section 5.1.1.3). Evidently complete equilibration is an unrealistic assumption, but current uncertainties in the correct value of k to employ are large, and it certainly depends on the scale of the impactor.

A further complication, which is usually ignored, is that only a fraction of the target mantle may initially equilibrate with the incoming core material. This process has the same effect as incomplete core equilibration on the subsequent isotopic evolution of the bulk mantle [*Sasaki and Abe*, 2007, *Morishima et al.*, 2013]. For bodies like Mars with a low $f^{\text{Hf/W}}$, this effect of incomplete mantle equilibration is unimportant [*Morishima et al.*, 2013], but for larger values of $f^{\text{Hf/W}}$, like the Earth's, it may be significant. Further study of this topic is required.

Determining a precise timescale for the formation of Earth's core is hampered by the tradeoff between equilibration factor and accretion rate. The Hf-W isotope systematics of the Earth alone, therefore, cannot precisely constrain the timescale of accretion and core formation. Nevertheless, Hf-W chronometry provides a strict lower limit of ~ 30 Myr after Solar System formation for the completion of Earth's accretion and core formation. There are at least three additional sources of information, which in principle can help to obtain a more detailed picture of the Earth's accretion. One, described in Section 5.2.3.2, is to use dynamical models to fix the accretion timescale, and then use $\Delta\epsilon_{\text{W}}$ to determine the

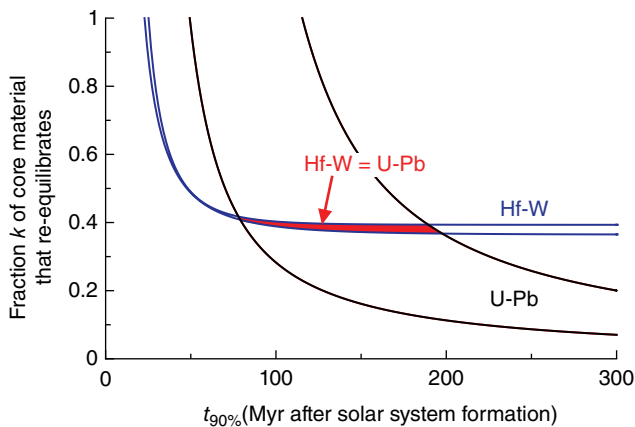


Figure 5.4 Tradeoff between re-equilibration fraction k and growth time for a continuous core formation model (equation 5.4) assuming exponentially decaying accretion [reproduced from *Kleine and Rudge*, 2011]. Here $t_{90\%}$ represents the time to 90% of the final mass in the exponential growth model, which would be equivalent to the time of the Moon-forming impact (see Section 5.2.5). To produce the same present-day tungsten anomaly of the BSE, higher degrees of re-equilibration require more rapid growth. Also shown are results of the U-Pb isotope system in the same accretion and core formation model (see Section 5.2.4.1). There is a region of overlap at $k \sim 0.4$, where both systems agree. For Hf-W the uncertainty arising from uncertainty in Hf/W of the BSE is shown; for U-Pb the uncertainty arising from the unknown bulk Pb isotope composition of the Earth is shown [see *Rudge et al.*, 2010].

degree of re-equilibration required. Another approach (Section 5.2.3.3) is to track both Hf-W isotope evolution and siderophile element partitioning in a given accretion model. Finally, the Hf-W chronometer can be combined with other chronometers having somewhat different characteristics, to derive an accretion scenario that matches all constraints (Section 5.2.4).

5.2.3.2. Combining Isotope Evolution Calculations with Dynamical Models

Various groups have started to incorporate isotopic evolution calculations into dynamical models of the final stages of terrestrial planet accretion [Nimmo and Agnor, 2006; Morishima *et al.*, 2013; Kobayashi and Dauphas, 2013]. If one assumes that these models provide an accurate description of how the Earth actually accreted, then the W isotopic evolution of the growing bodies can be calculated and the extent of re-equilibration determined by matching the Earth's observed ^{182}W anomaly.

An example of carrying out isotopic calculations on accretion simulations is shown in Figure 5.5. Across these eight simulations [O'Brien *et al.*, 2006], the time at which a body exceeds 90% of its final mass ranges from 4 to 63 Myr, and the final giant impact can occur as early as 14 Myr and as late as 232 Myr. Although these two extremes are not consistent with isotopic constraints on Earth's accretion timescale (see above), this range of values nevertheless serves to illustrate the highly stochastic nature of the accretion process.

Figure 5.5 plots the average mantle tungsten anomaly across all Earth-mass bodies as a function of equilibration fraction k , where k is assumed constant throughout.

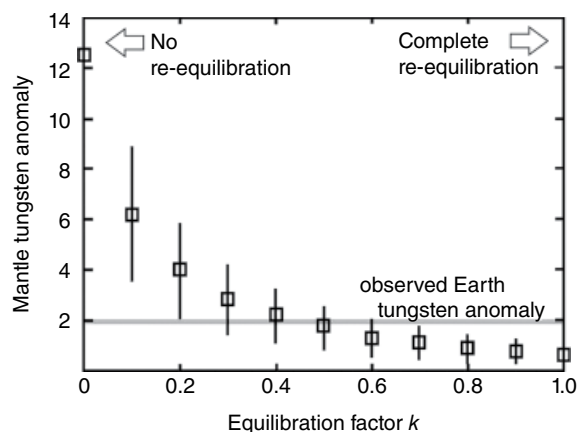


Figure 5.5 Mean mantle tungsten anomaly $\Delta\epsilon_{\text{W}}$ as a function of equilibration factor k based on tracking the isotopic evolution of bodies in a suite of N-body accretion models. Constant tungsten partitioning coefficients are assumed. Reproduced from Nimmo *et al.* [2010].

As expected, lower degrees of equilibration result in higher tungsten anomalies, and vice versa. On average, Earth-like tungsten anomalies are obtained for intermediate degrees of equilibration ($k=0.3-0.7$).

An advantage of this approach is that it tracks the isotopic history of each body; as a result, there is no need (unlike analytical models) to assume that all bodies follow an identical isotopic evolution. It is also easy to explore the consequences of allowing k or the partitioning behavior of Hf and W to vary as a function of time, radial position, or body size. Perhaps the biggest disadvantage of this approach is that accretion is stochastic so that large numbers of simulations need to be run [e.g., Fischer and Ciesla, 2014], and then only probabilistic statements can be made.

This approach is also only as reliable as the accretion models themselves. For instance, recent accretion models have started to investigate the effects of imperfect accretion (Section 5.1.1.1), which can change both the overall accretion timescale and the bulk chemistry of surviving bodies. Preliminary investigations [Dwyer *et al.*, 2015] suggest that the latter effect is relatively minor for Earth-mass planets, because of the averaging effects of multiple large impacts. However, the overall increase in accretion timescale requires k to decrease slightly (to 0.2–0.6) to match the observed tungsten anomaly of the Earth's mantle.

Overall, results based on accretion simulations suggest that the Earth accreted material that (on average) underwent intermediate degrees of re-equilibration ($k\sim 0.5$). In reality, larger impactors probably suffered less re-equilibration and smaller ones more, but the details are highly uncertain.

5.2.3.3. How Did the Partitioning Behavior of Siderophile Elements Evolve During Accretion?

In the models discussed up to this point, it is assumed that the fractionation of Hf from W during core formation is time-independent (i.e., the partition coefficients D_{Hf} and D_{W} are constant). This is a convenient simplification because D_{Hf} and D_{W} can be calculated, given the known mantle Hf/W ratio and iron:silicate ratio of the Earth. However, reality is clearly more complicated because the partition coefficient of W varies with pressure (P), temperature (T), and oxygen fugacity ($f\text{O}_2$), and thus will have changed as accretion proceeded. For instance, the relevant partition coefficients apply at the point when iron-silicate equilibration ceases; thus, for small liquid iron blobs sinking through a magma ocean, the relevant P,T conditions are those at the base of the magma ocean. Since the depth of the magma ocean probably increased as the Earth grew, the P,T conditions of metal-silicate equilibration and with them the partitioning behavior of W will have also changed. Furthermore, D_{W} also is

strongly dependent on oxygen fugacity, so that W becomes less siderophile under oxidizing conditions [Cottrell *et al.*, 2009; Wade *et al.*, 2013]. For instance, the much lower Hf/W ratio of bulk silicate Mars compared to the Earth's mantle (Table 5.1) probably reflects core formation under more oxidizing conditions.

The characterization of partition coefficients at the relevant P, T and fO_2 conditions is an ongoing challenge [e.g., Siebert *et al.*, 2013]. The result is non-uniqueness. Various groups have made different assumptions about the evolution of P, T and fO_2 , all of which are capable of matching the inferred mantle siderophile concentrations. Some groups favor progressively oxidizing conditions [e.g., Wade and Wood, 2005; Rubie *et al.*, 2011], while others advocate oxidized conditions throughout [Siebert *et al.*, 2013]. These different scenarios make quite different predictions about the nature of the light elements in the core, and can thus in theory be tested. Further discussion of this topic may be found in Chapter 6.

Obviously, any successful accretion and core formation model must not only satisfy the Hf-W isotope systematics but also the observed siderophile element depletions in the Earth's mantle. This makes combining siderophile element and Hf-W isotope systematics a promising approach for more tightly constraining the core formation history of the Earth. Such a combined approach may in particular help to assess the degree of re-equilibration during metal segregation within the Earth. However, Rudge *et al.* [2010] showed that the siderophile element and Hf-W isotope systematics of the Earth's mantle are equally consistent with 100% re-equilibration as well as with ~40% re-equilibration during core formation, depending on the growth history assumed. This result may be compared with the 30 to 70% range in re-equilibration factors derived from dynamical models (Fig. 5.5). Ultimately, although it is clearly essential to consider siderophile element partitioning and Hf-W isotope systematics together, this approach so far only provides limited constraints on the degree of metal-silicate re-equilibration, the most important parameter for Hf-W chronometry of core formation in the Earth.

5.2.4. Other Chronometers

Although the Hf-W system represents the best single core formation chronometer, it does suffer from limitations. An alternative approach to obtain better constraints on the timing of core formation is to employ multiple isotopic systems. For the Earth, the three most relevant systems are the U-Pb, Pd-Ag, and I-Xe. Both U-Pb and Pd-Ag are sensitive to core formation, but interpretation is complicated by other factors, and the I-Xe system is sensitive to degassing, which is often assumed to occur as a result of late-stage giant impacts.

5.2.4.1. Evidence from Combined Hf-W and U-Pb Isotope Systematics

The U-Pb isotope system was the first to provide a precise age for the Earth [Patterson, 1956]. The principle of this system to date core formation in the Earth is as follows. In a plot of $^{207}\text{Pb}/^{204}\text{Pb}$ vs. $^{206}\text{Pb}/^{204}\text{Pb}$, all estimates for the Pb isotope composition of the bulk silicate Earth plot to the right of the geochron (Fig. 5.6), indicating that the Earth's mantle underwent a major U/Pb fractionation event some time after Solar System formation. Most estimates for the Pb isotope composition of the BSE return ages of between ~50 and ~150 Myr after the start of the Solar System [see summary in Rudge *et al.*, 2010 and Wood and Halliday, 2010]. All the Pb-Pb ages have in common that they are younger than the Hf-W model age for core formation in the Earth. The disparate Pb-Pb and Hf-W ages of the Earth's core have been interpreted to reflect disequilibrium during core formation [Halliday, 2004; Kleine *et al.*, 2004; Rudge *et al.*, 2010; Kleine and Rudge, 2011]. It is noteworthy that the Hf-W and U-Pb isotope systematics provide consistent $t_{90\%}$ timescales of 80–200 Myr for a degree of re-equilibration of ~40% (Fig. 5.4), in reasonable agreement with the range obtained from dynamical models.

The apparent discrepancy between the Hf-W and Pb-Pb model ages may alternatively reflect the fact that Earth's accretion is not correctly described by the exponential accretion model (cf. Fig. 5.1). Using a more general growth model shows that the Hf-W and Pb-Pb

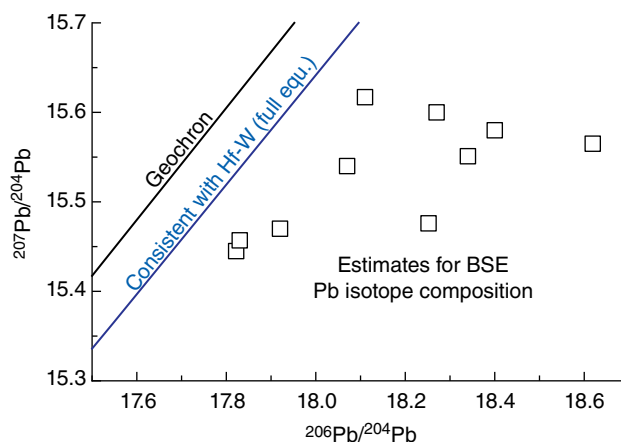


Figure 5.6 Comparison of estimated bulk silicate Earth (BSE) lead isotope ratios with those expected for a zero-age reservoir as given by the Geochron. Blue line indicates loci of data points for which the timing obtained from Hf-W and U-Pb isotope systematics in the exponential growth model (equation 5.4) would be consistent, assuming full equilibration. For estimates of BSE compositions see Rudge *et al.* [2010].

ages of the Earth's core can be reconciled if the Earth grew rapidly initially, with $t_{63\%}$ between 0.4 and 2.5 Myr, followed by a much more protracted accretion period terminated by a 'late' giant impact at ~ 100 Myr [Rudge *et al.*, 2010].

Although the Hf-W and Pb-Pb ages of the Earth can reasonably well be brought into agreement (Fig. 5.4), the significance of Pb-Pb age is debated, and it has been argued that the Pb-Pb age does not date core formation but the arrival of late veneer some time after core formation [Albarede, 2009]. In this case, core formation would have occurred earlier than given by the Pb-Pb age. However, this model would require large additions ($\sim 4\%$) of primitive chondritic material to the Earth after the cessation of core formation, inconsistent with the $\sim 0.5\%$ mass of the late veneer derived from abundances of highly siderophile elements in the Earth's mantle [Wood *et al.*, 2010]. To overcome this problem, Albarede *et al.* [2013] proposed that during addition of the late veneer most of the metal entered Earth's core, thereby allowing for a larger mass to be added.

However, as argued above, core formation in the Earth almost certainly involved some disequilibrium, in which case the Hf-W and Pb-Pb ages for core formation are in good agreement (Fig. 5.4). Thus, there is no need to invoke more complicated models in which the two systems date distinct events. Moreover, an apparent disparity between the Hf-W and Pb-Pb ages only arises if complete re-equilibration and a certain growth model (the exponential model) are assumed. Given the stochastic nature of accretion and the likelihood of disequilibrium during giant impacts, these two assumptions are probably not valid. Thus, the most straightforward interpretation of the Hf-W and Pb-Pb systematics is that both provide constraints on the timing of core formation. The strength of using both systems lies in the fact that they date different stages of core formation because of their very different half-lives [Rudge *et al.*, 2010; Kleine and Rudge, 2011]. Whereas Hf-W as a short-lived nuclide system mainly constrains the early stages of accretion and core formation; therefore, it provides little information on the end of core formation. This is because the Hf-W system becomes extinct after *ca.* 60 Myr and so the W isotope composition of the mantle is mainly set by very early Hf/W fractionation. In contrast, the long-lived Pb-Pb system provides little information on the early stages of accretion and core formation but mainly constrains the end of core formation. This is because the present-day Pb isotope composition of the mantle mainly records the final U/Pb fractionation and subsequent decay over *ca.* 4.4 Ga. The Hf-W and Pb-Pb systems are mutually consistent with an end of core formation at ~ 80 – 200 Myr after Solar System formation (Fig. 5.4).

5.2.4.2. Evidence from Pd-Ag Systematics

The Pd/Ag system is in some ways similar to the Hf/W system. ^{107}Pd decays to ^{107}Ag with a half-life of 6.5 Myr, and Pd partitions more strongly into the core than Ag. As a result, early core formation results in a deficit in ^{107}Ag relative to undifferentiated material. However, the major difficulty in using Pd-Ag isotope systematics to constrain the timescales of core formation in the Earth is that Ag is moderately volatile, so that the Pd/Ag ratio of the bulk Earth is not known. Nevertheless, when combined with other independent constraints on the timing of core formation, Pd-Ag systematics are useful to constrain the timing of volatile delivery to the Earth.

The Ag isotope composition of the bulk silicate Earth (BSE) is roughly the same as that of chondritic material [Schönbächler *et al.*, 2010]. Given that on average the Earth is more depleted in volatiles than chondrites, the bulk Earth should have a more radiogenic ϵ_{Ag} than chondrites. Thus, relative to the expected Ag isotope composition of the bulk Earth, the BSE exhibits a ^{107}Ag deficit, which would require a rapid core formation timescale (two-stage age of less than 10 Myr). This result is inconsistent with the Hf-W constraints, which yields a two-stage age of roughly 30 Myr. This apparent discrepancy can be accounted for by invoking a change in the nature of the accreting material, initially volatile-depleted and later volatile-rich [Schönbächler *et al.*, 2010]. In this classical heterogeneous accretion model, the Ag isotope composition of the BSE is almost entirely dominated by the later accreted material, which on average had chondritic Pd/Ag and ^{107}Ag abundances. This model is consistent with numerical modeling that shows a progressive radial expansion of the feeding zone (see Section 5.1.1.1), thus delivering more distant (and thus more volatile-rich) impactors at later times. If the volatile-depleted and volatile-enriched impactors are reduced and oxidized, respectively, then this scenario is also consistent with the concentrations of siderophile elements in the BSE [Wade and Wood, 2005; Rubie *et al.*, 2011]. Thus, although the Pd-Ag systematics provide no additional constraints on the core formation timescale, they seem to require that the Earth accreted a mix of early volatile-depleted and later volatile-enriched material.

The mass fraction of volatile-rich material added to account for the chondritic ^{107}Ag of the BSE is significant, and cannot merely be the ~ 0.5 wt% "late veneer," which is thought to have been added after core formation was effectively complete (see chapter 4). A pre-late-veener Earth that already had a significant volatile budget is also consistent with estimates based on S, Se, and Te concentrations [Wang and Becker, 2013].

5.2.5. Timing of Moon-forming Impact

The final large impactor to strike the Earth was probably the one that formed the Moon. This final impact thus represents the effective end of core formation on Earth. As a result, evidence from the Moon can be used to help determine the timescale of terrestrial core formation.

The bulk silicate Moon and Earth appear to have very similar ϵ_w and this has been interpreted to indicate a 'late' formation of the Moon, more than ~ 50 Myr after the start of the Solar System [Touboul *et al.*, 2007, 2009]. The interpretation relies on the assumption that the Moon formed from terrestrial mantle material and as such had the same initial W isotope composition as the Earth's mantle at the time of the giant impact. If the Hf/W ratios of the bulk silicate Moon and bulk silicate Earth are different, then their similar W isotope compositions require formation of the Moon after extinction of ^{182}Hf , that is, after ~ 50 Myr. There is currently debate as to whether the Hf/W ratios of the lunar and terrestrial mantles are distinct or not [e.g., König *et al.*, 2011]. However, two observations indicate that it is unlikely that they are exactly identical. First, the Hf/W ratio of the bulk silicate Moon was established by lunar core formation and, hence, is not simply inherited from the proto-Earth's mantle. Second, the conditions of core formation in the Moon and Earth were likely different and so there is no reason to assume that the lunar and terrestrial mantles have the same Hf/W ratio. Thus, the most straightforward interpretation of the similar ^{182}W anomalies of the Earth's mantle and Moon is that the Moon is 'young.' Note that there seems to be a small difference between the ϵ_w of the present-day bulk silicate Earth and the Moon (see Section 5.2.2). This difference most likely reflects the different amounts of post-core formation additions of material to both bodies (the "late veneer") [Kruijer *et al.*, 2015; Walker, 2014]. The amount of late veneer material added to the Earth's mantle has also been used to argue for a young Moon based on dynamical arguments [Jacobson *et al.*, 2014].

An alternative approach for determining the age of the Moon is to date the formation of lunar crustal rocks, the ferroan anorthosites. These are thought to have formed as flotation cumulates on top of the lunar magma ocean, and their age should thus approximate (and certainly not precede) the age of the Moon. This is because the lunar magma ocean, which formed in the immediate aftermath of the giant impact, is expected to have cooled very rapidly, at least until the formation of the first insulating crust. Most ferroan anorthosites dated so far have ages around ~ 4.45 Ga [Norman *et al.*, 2003; Nyquist *et al.*, 2006]; however, a recent study reported a very precise age of 4360 ± 3 Ma for ferroan anorthosite 60025 [Borg *et al.*, 2011]. Boyet *et al.* [2015] argued that the oldest ferroan anorthosite has a crystallization age of between ~ 4.50

and ~ 4.44 Ga, and that younger ages may reflect resetting or that not all anorthosites are flotation cumulate. Finally, chronological evidence from Mg-suite crustal rocks indicate a major period of crust formation on the Moon at ~ 4.4 Ga [Carlson *et al.*, 2014]. Collectively, there does not seem to be evidence for significant crust formation on the Moon prior to ~ 4.45 Ga, implying that either the Moon did not form earlier than ~ 100 Myr or that the ferroan anorthosites are not flotation cumulates of the lunar magma ocean.

Additional evidence arises from the I-Xe system. The existence of isotopically distinct Xe reservoirs within the BSE indicates differentiation prior to 100 Myr [Mukhopadhyay, 2012] and may suggest two episodes of outgassing at ~ 20 – 50 Myr and ~ 100 Myr [Pepin and Porcelli, 2006]. If the Moon-forming impact occurred more recently than 100 Myr, then it must not have destroyed pre-existing mantle heterogeneities, a conclusion also suggested by the survival of early-established ϵ_w anomalies [Touboul *et al.*, 2012].

5.2.6. Summary: When Did Core Formation Occur?

At this point, it should be obvious that for an Earth-mass body, the idea of there being a single instant of core formation is inappropriate. Instead, core formation proceeded in the same manner as planetary growth, episodically, in large, stochastic increments (Fig 5.1). Nonetheless, some bounds can be established. Based on Figure 5.4, core formation cannot have ended prior to 30 Myr, and based on the apparent timing of the Moon-forming impact, it is unlikely to have continued past 150–200 Myr. These isotopically-derived limits are consistent with typical timescales derived from dynamical N-body simulations. Indeed, the good agreement between these two wildly different ways of quantifying the Earth's accretion timescale represents a major success in geosciences.

A more precise picture of how the Earth grew is currently elusive and may remain so. The available isotopic clocks are hampered by the problem of partial equilibration (Section 5.2.3.1), and this is particularly true for the Hf-W system. Scenarios that satisfy several different isotopic systems simultaneously can help overcome this issue. For instance, combining Hf-W and U-Pb isotope systematics provides a consistent age for the Earth of 80–200 Myr if the degree of metal-silicate re-equilibration during core formation was only $\sim 40\%$ on average (Section 5.2.4.1). This age is also in good agreement with ages of lunar ferroan anorthosites, which should closely approximate the formation of the Moon (provided they are flotation cumulates of the lunar magma ocean) and hence the termination of the main stages of Earth's accretion.

The timescales for the accretion of the Earth indicated by these isotopic approaches are roughly consistent with

the results of dynamical models. Similarly, Pd-Ag isotope systematics seem to require that the Earth accreted from volatile-poor material initially, followed by a shift to more volatile-rich material during the later stages of accretion. This observation is also consistent with some dynamical simulations showing that more volatile-rich bodies located further away from the sun were added to the Earth during the late stages of accretion [O'Brien *et al.*, 2014]. Dynamical models themselves are inevitably stochastic and are constantly under revision. Nonetheless, testing the outcomes of such models with the isotopic constraints is an important consistency test for any model and as such can provide powerful new constraints. Such combined studies are likely to become increasingly standard practice going forward [Nimmo and Agnor, 2006; Kobayashi and Dauphas, 2013; Morishima *et al.*, 2013].

5.3. SUMMARY AND CONCLUSIONS

The Earth's core formed via a series of high-energy collisions with already-differentiated objects, resulting in several distinct magma ocean epochs. The cores of these impactors probably underwent only limited emulsification and moderate (~50%) isotopic re-equilibration with the target mantle during the collision. Later impactors likely originated from more distant regions of the inner Solar System and were plausibly more volatile-rich and more oxidized than earlier impactors. Dynamical models and short-lived isotopes provide a mutually self-consistent, albeit approximate, chronology: terrestrial core formation took more than 30 Myr, but less than about 200 Myr, to complete.

Figure 5.7 is a summary sketch of how differentiation and core formation are likely to have proceeded with

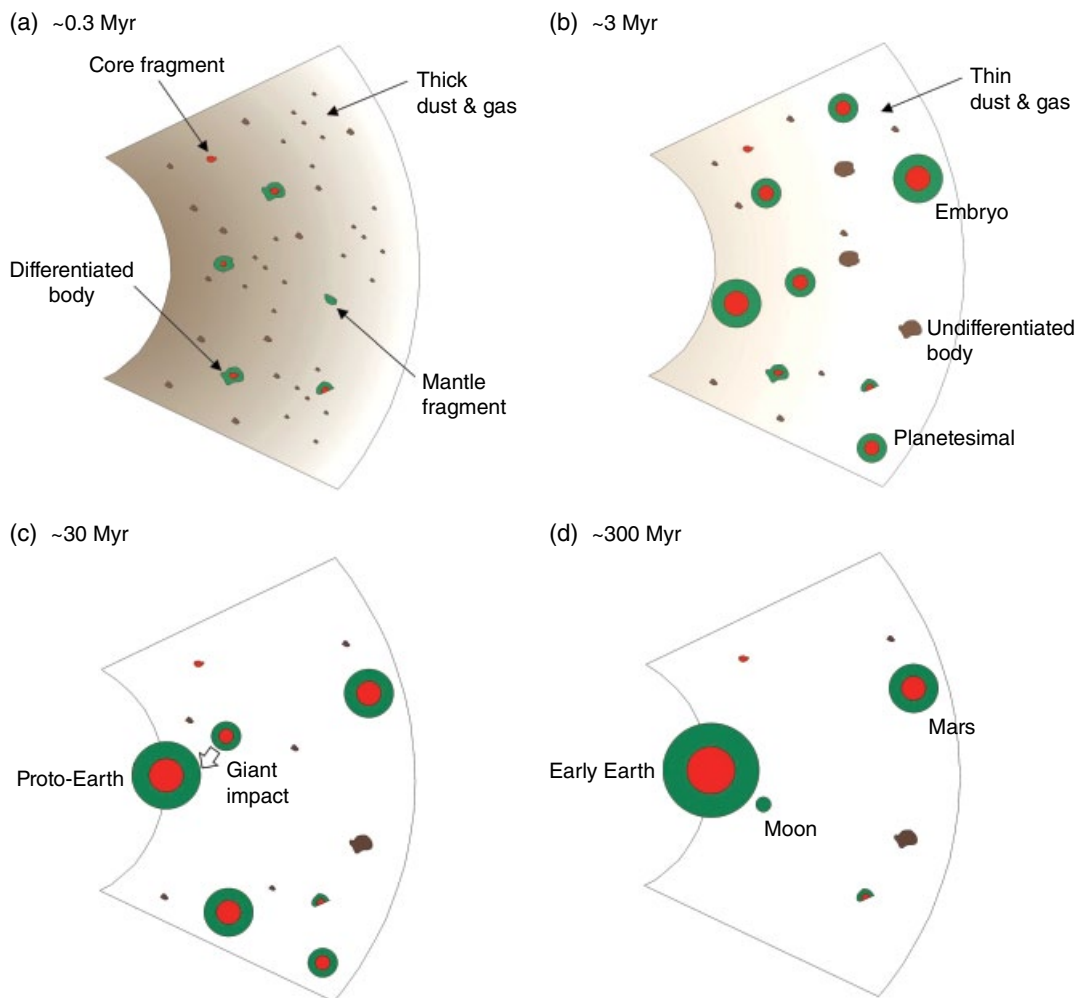


Figure 5.7 Schematic view looking down on the ecliptic, centered at about 1AU, at different stages during the accretion of the terrestrial planets. Brown, green, and red indicate undifferentiated, silicate, and iron materials, respectively. ^{26}Al is effectively extinct by 3 Myr after CAI; at roughly the same time any remaining gas and dust is swept away by young stellar activity. Timescales are only approximate.

time. By ~ 0.3 Myr after Solar System formation, some bodies had grown large enough (>30 km diameter) to undergo melting and core formation via ^{26}Al decay (Fig. 5.7a). Collisional disruption will have resulted in core and mantle fragments being produced. At ~ 3 Myr, the nebular gas and dust were dissipating, and ^{26}Al was effectively extinct. Differentiated, Moon- to Mars-sized planetesimals and embryos had formed, while more slowly growing, smaller bodies avoided differentiating via either ^{26}Al decay or gravitational energy release (Fig. 5.7b). The growth of Mars may have effectively stalled at this point. At ~ 30 Myr, late-stage accretion involving massive collisions between differentiated protoplanets was taking place (Fig. 5.7c). By ~ 300 Myr, the Earth and Moon had finished forming and the neighborhood around 1 AU approximately resembled its current configuration (Fig. 5.7d).

Many aspects of core formation remain enigmatic. In particular, the fluid dynamics of an impactor core passing through the target mantle is very poorly understood, and yet is crucial for predicting the extent of re-equilibration (Section 5.2.3.1). Only very recently has the inefficient nature of accretion become obvious (Section 5.1.1.1). Exploration of the effect of including more realistic accretion physics on the isotopic evolution of terrestrial bodies has barely begun (Dwyer *et al.*, 2015). Partitioning behavior at high pressures is only imperfectly understood but can have a significant effect on the conditions inferred to characterize core formation (Section 5.2.3.3).

Remedying these lacunae in our knowledge will certainly improve our understanding of core formation. Ever more precise isotopic measurements and ever more sophisticated accretion simulations will also improve our understanding. Ultimately, however, the biggest advances are likely to arise from a combination of these two latter approaches. Like many problems in Earth sciences, the perspectives of both geochemists and geophysicists will be required to elucidate exactly how the core formed.

ACKNOWLEDGMENTS

We thank Dave Rubie and Qing-Zhu Yin for thoughtful comments that improved this manuscript. Partial support was provided by NASA-NNX11AK60G and an ERC Advanced Grant “ACCRETE” (contract number 290568).

REFERENCES

- Abe, Y. and T. Matsui (1986), Early evolution of the Earth—accretion, atmosphere formation and thermal history, *J. Geophys. Res.*, *91*, E291–E302.
- Agnor, C.B., R. M. Canup, and H. F. Levison (1999), On the character and consequences of large impacts in the late stage of terrestrial planet formation, *Icarus*, *142*, 219–237.
- Albarede, F. (2009), Volatile accretion history of the terrestrial planets and dynamic implications, *Nature*, *461*, 1227–1233.
- Albarede, F., C. Ballhaus, J. Blichert-Toft, C. T. Lee, B. Marty, F. Moynier, and Q.Z. Yin (2013), Asteroidal impacts and the origin of terrestrial and lunar volatiles, *Icarus*, *222*, 44–52.
- Alfe, D., M. J. Gillan, and G. D. Price (2002), Ab initio chemical potentials of solid and liquid solutions and the chemistry of the Earth’s core, *J. Chem. Phys.*, *116*, 7127–7136.
- Araki, T. *et al.* (2005), Experimental investigations of geologically produced antineutrinos with KamLAND, *Nature*, *436*, 499–503.
- Asphaug, E., C.B. Agnor and Q. Williams (2006), Hit-and-run planetary collisions, *Nature*, *439*, 155–160.
- Bond, J. C., D. S. Lauretta, and D. P. O’Brien (2010), Making the Earth: Combining dynamics and chemistry in the solar system, *Icarus*, *205*, 321–337.
- Borg, L.E., J. N. Connelly, M. Boyet, and R. W. Carlson (2011), Chronological evidence that the Moon is either young or did not have a global magma ocean, *Nature*, *477*, 70–72.
- Bouhifd, M. A., L. Gautron, N. Bolfan-Casanova, V. Malavergne, T. Hammouda, D. Andraut, and A. P. Jephcoat (2007), Potassium partitioning into molten alloys at high pressure: Implications for Earth’s core, *Phys. Earth Planet. Inter.*, *160*, 22–33.
- Boyet, M., R. W. Carlson, L. E. Borg, and M. Horan (2015), Sm-Nd systematics of lunar ferroan anorthositic suite rocks: constraints on lunar crust formation. *Geochim. Cosmochim. Acta.*, *148*, 203–218.
- Burkhardt, C., T. Kleine, N. Dauphas, and R. Wieler (2012), Nucleosynthetic tungsten isotope anomalies in acid leachates of the Murchison chondrite: implications for hafnium-tungsten chronometry. *Astrophys. J. Lett.*, *753*, L6.
- Canup, R. M. (2004), Simulations of a late lunar-forming impact, *Icarus*, *168*, 433–456.
- Canup, R. M. (2012), Forming a Moon with an Earth-like composition via a giant impact, *Science*, *338*, 1052–1055.
- Carlson, R. W., L. E. Borg, A. M. Gaffney, and M. Boyet (2014), Rb-Sr, Sm-Nd and Lu-Hf isotope systematics of the lunar Mg-suite: the age of the lunar crust and its relation to the time of Moon formation. *Phil. Trans. R. Soc. A*, *372*, 20130246.
- Chambers, J. (2010), Terrestrial planet formation, in *Exoplanets*, S. Seager, Ed., pp. 297–318, Univ. Ariz. Press.
- Chambers, J. E. (2013), Late-stage planetary accretion including hit-and-run collisions and fragmentation, *Icarus*, *224*, 43–56.
- Corgne, A., S. Keshav, Y. W. Fei, and W. F. McDonough (2007), How much potassium is in the Earth’s core? New insights from partitioning experiments, *Earth Planet. Sci. Lett.*, *256*, 567–576.
- Cottrell, E., M. J. Walter, and D. Walker (2009), Metal-silicate partitioning of tungsten at high pressure and temperature: Implications for equilibrium core formation in Earth, *Earth Planet. Sci. Lett.*, *281*, 275–287.
- Cuk, M. and S. T. Stewart, Making the Moon from a fast-spinning Earth: A giant impact followed by resonant despinning (2012), *Science*, *338*, 1047–1052.
- Dahl, T. and D. J. Stevenson (2010), Turbulent mixing of metal and silicate during planet accretion—An interpretation of the Hf-W chronometer, *Earth Planet. Sci. Lett.*, *295*, 177–186.

- Dauphas, N. and A. Pourmand (2011), Hf-W-Th evidence for rapid growth of Mars and its status as a planetary embryo, *Nature*, *473*, 489–491.
- Dauphas, N., C. Burkhardt, P. H. Warren, and F.-Z. Teng (2014), Geochemical arguments for an Earth-like Moon-forming impactor. *Phil. Trans. R. Soc. A*, *372*, 20130244.
- Debaille, V., A. D. Brandon, Q. Z. Yin, and B. Jacobsen (2007), Coupled Nd-142-Nd-143 evidence for a protracted magma ocean in Mars, *Nature*, *450*, 525–528.
- Deguen, R., P. Olson, and P. Cardin (2011), Experiments on turbulent metal-silicate mixing in a magma ocean, *Earth Planet. Sci. Lett.*, *310*, 303–313.
- Dwyer, C. A., F. Nimmo, and J. E. Chambers (2015), Bulk chemical and isotopic consequences of incomplete accretion during planet formation, *Icarus*, *245*, 145–152.
- Elkins-Tanton, L. T., B. P. Weiss, and M. T. Zuber (2011), Chondrites as samples of differentiated planetesimals, *Earth Planet. Sci. Lett.*, *305*, 1–10.
- Fischer, R. A. and F. J. Ciesla (2014), Dynamics of the terrestrial planets from a large number of N-body simulations, *Earth Planet. Sci. Lett.*, *392*, 28–38.
- Foley, C. N., M. Wadhwa, L. E. Borg, P. E. Janney, R. Hines, and T. L. Grove (2005), The early differentiation history of Mars from W-182-Nd-142 isotope systematic in the SNC meteorites, *Geochim. Cosmochim. Acta.*, *69*, 4557–4571.
- Georg, R. B., A. N. Halliday, E. A. Schauble, and B. C. Reynolds (2007), Silicon in the Earth's core, *Nature*, *447*, 1102–1106.
- Halliday, A. N. (2004), Mixing, volatile loss and compositional change during impact-driven accretion of the Earth, *Nature*, *427*, 505–509.
- Huang, H. F., Y. W. Fei, L. C. Cai, F. Q. Jing, X. J. Hu, H. S. Xie, L. M. Zhang, and Z. Z. Gong (2011), Evidence for an oxygen-depleted liquid outer core of the Earth, *Nature*, *479*, 513–516.
- Jacobsen, S. B. (2005), The Hf-W isotopic system and the origin of the Earth and Moon, *Ann. Rev. Earth Planet. Sci.*, *33*, 531–570.
- Jacobson, S. A., A. Morbidelli, S. N. Raymond, D. P. O'Brien, K. J. Walsh, and D. C. Rubie (2014), Highly siderophile elements in Earth's mantle as a clock for the Moon-forming impact. *Nature*, *508*, 84–87.
- Kleine, T. and J. F. Rudge (2011), Chronometry of meteorites and the formation of the Earth and Moon, *Elements*, *7*, 41–46.
- Kleine, T., C. Münker, K. Mezger, and H. Palme (2002), Rapid accretion and early core formation on asteroids and terrestrial planets from Hf-W chronometry. *Nature*, *418*, 952–955.
- Kleine, T., K. Mezger, H. Palme, and C. Münker (2004), The W isotope evolution of the bulk silicate Earth: constraints on the timing and mechanisms of core formation and accretion, *Earth Planet. Sci. Lett.*, *228*, 109–123.
- Kleine, T., M. Touboul, B. Bourdon, F. Nimmo, K. Mezger, H. Palme, S. B. Jacobsen, Q. Z. Yin, and A. N. Halliday (2009), Hf-W chronology of the accretion and early evolution of asteroids and terrestrial planets, *Geochim. Cosmochim. Acta.*, *73*, 5150–5188.
- Kleine, T., U. Hans, A. J. Irving, and B. Bourdon (2012), Chronology of the angrite parent body and implications for core formation in protoplanets, *Geochim. Cosmochim. Acta.*, *84*, 186–203.
- Kobayashi, H. and N. Dauphas (2013), Small planetesimals in a massive disk formed Mars, *Icarus*, *225*, 122–130.
- Kokubo, E. and S. Ida (1998), Oligarchic growth of protoplanets, *Icarus*, *131*, 171–178.
- Kokubo, E. and H. Genda (2010), Formation of terrestrial planets from protoplanets under a realistic accretion condition, *Astrophys. J. Lett.*, *714*, 21–25.
- Kruijjer, T. S., M. Fischer-Goedde, T. Kleine, P. Sprung, I. Leya, and R. Wieler (2013), Neutron capture on Pt isotopes in iron meteorites and the Hf-W chronology of core formation in planetesimals, *Earth Planet. Sci. Lett.*, *361*, 162–172.
- Kruijjer, T. S., M. Touboul, M. Fischer-Gödde, K. R. Bermingham, R. J. Walker, and T. Kleine (2014a), Protracted core formation and rapid accretion of protoplanets. *Science*, *344*, 1150–1154.
- Kruijjer, T. S., T. Kleine, M. Fischer-Gödde, C. Burkhardt, and Wieler, R. (2014b), Nucleosynthetic W isotope anomalies and Hf-W chronometry of Ca-Al-rich inclusions. *Earth Planet. Sci. Lett.*, *403*, 317–327.
- Kruijjer, T. S., T. Kleine, M. Fischer-Gödde, and P. Sprung (2015), Lunar tungsten isotopic evidence for the late veneer. *Nature*, *520*, 534–537.
- McCoy, T. J., D. W. Mittlefehldt, and L. Wilson (2006), Asteroid differentiation, in *Meteorites and the early solar system II*, Univ. Ariz. Press, pp. 733–745.
- McDonough, W. F. (2003), Compositional model for the Earth's core, in *Treatise on Geochemistry*, pp. 517–586.
- McKenzie, D. (1984), The generation and compaction of partially molten rock, *J. Petrology*, *25*, 713–765.
- Mezger, K., V. Debaille, and T. Kleine, (2013), Core formation and mantle differentiation on Mars. *Space Sci. Rev.*, *174*, 27–48.
- Mittlefehldt, D. W., T. J. McCoy, C. A. Goodrich, and A. Kracher (1998), Non-chondritic meteorites form asteroidal bodies. In *Planetary Materials* (Ed. J.J. Papike). Rev. Mineral., Mineralogical Society of America, Washington DC, vol. 36, chap. 4, pp. 4–1 – 4–495.
- Morard, G., J. Siebert, D. Andrault, N. Guignot, G. Garbarino, F. Guyot, and D. Antonangeli (2013), The Earth's core composition from high pressure density measurements of liquid iron alloys, *Earth Planet. Sci. Lett.*, *373*, 169–178.
- Morbidelli, A., J. I. Lunine, D. P. O'Brien, S. N. Raymond, and K. J. Walsh (2012), Building terrestrial planets, *Ann. Rev. Earth Planet. Sci.*, *40*, 251–275.
- Morishima, R., G. J. Golabek, and H. Samuel (2013), N-body simulations of oligarchic growth of Mars: Implications for Hf-W chronology, *Earth Planet. Sci. Lett.*, *366*, 6–16.
- Mukhopadhyay, S. (2012), Early differentiation and volatile accretion recorded in deep-mantle neon and xenon, *Nature*, *486*, 101–104.
- Nimmo, F. (2015), Thermal and compositional evolution of the core, *Treatise Geophys.*, *9*, 201–209.
- Nimmo, F. and T. Kleine (2007), How rapidly did Mars accrete? *Uncertainties in the Hf-W timing of core formation*, *Icarus*, *191*, 497–504.
- Nimmo, F. and C. B. Agnor (2006), Isotopic outcomes of N-body accretion simulations: Constraints on equilibration processes during large impacts from Hf/W observations, *Earth Planet. Sci. Lett.*, *243*, 26–43.

- Nimmo, F., D. P. O'Brien, and T. Kleine (2010), Tungsten isotopic evolution during late-stage accretion: Constraints on Earth-Moon equilibration, *Earth Planet. Sci. Lett.*, *292*, 363–370.
- Norman, M. D., L. E. Borg, L. E. Nyquist, and D. D. Bogard (2003), Chronology, geochemistry and petrology of a ferroan noritic anorthosite clast from Descartes breccias 67215: Clues to the age, origin, structure and impact history of the lunar crust, *Meteorit. Planet. Sci.*, *38*, 645–661.
- Nyquist, L., D. Bogard, A. Yamaguchi, C.-Y. Shih, Y. Karouji, M. Ebihara, Y. Reese, D. Garrison, G. McKay, and H. Takeda (2006), Feldspathic clasts in Yamato-86032L: Remnants of the lunar crust with implications for its formation and impact history, *Geochim. Cosmochim. Acta.*, *70*, 5990–6015.
- O'Brien, D. P., A. Morbidelli, and H.F. Levison (2006), Terrestrial planet formation with strong dynamical friction, *Icarus*, *184*, 39–58.
- O'Brien, D. P., K. J. Walsh, A. Morbidelli, S. N. Raymond, and A. M. Mandell (2014), Water delivery and giant impacts in the 'Grand Tack' scenario, *Icarus*, *239*, 74–84.
- O'Neill, H.S.C and H. Palme (2008), Collisional erosion and the non-chondritic composition of the terrestrial planets, *Phil. Trans. R. Soc. Lond. A*, *366*, 4205–4238.
- Patterson, C. (1956), Age of meteorites and the Earth, *Geochim. Cosmochim. Acta.*, *10*, 230–237.
- Pepin, R.O. and D. Porcelli (2006), Xenon isotope systematic, giant impacts, and mantle degassing on the early Earth, *Earth Planet. Sci. Lett.*, *250*, 470–485.
- Poirier, J.-P. (1994), Light elements in the Earth's outer core: A critical review, *Phys. Earth Planet. Inter.*, *85*, 319–337.
- Raymond, S. N., T. Quinn, and J. I. Lunine (2006), High resolution simulations of the final assembly of Earth-like planets I. *Terrestrial accretion and dynamics*, *Icarus*, *183*, 265–282.
- Ricard, Y., O. Sramek, and F. Dubuffet (2009), A multi-phase model of runaway core-mantle segregation in planetary embryos, *Earth Planet. Sci. Lett.*, *284*, 144–150.
- Ricolleau, A., Y. W. Fei, A. Corgne, J. Siebert, and J. Badro (2011), Oxygen and silicon contents of Earth's core from high pressure metal-silicate partitioning experiments, *Earth Planet. Sci. Lett.*, *310*, 409–412.
- Rubie, D. C., F. Nimmo, and H. J. Melosh (2007), Formation of the Earth's core, in *Treatise Geophysics*, *9*, 43–79.
- Rubie, D. C., H. H. Melosh, J. E. Reid, C. Lieske, and K. Righter (2003), Mechanisms of metal-silicate equilibration in the terrestrial magma ocean, *Earth Planet. Sci. Lett.*, *205*, 239–255.
- Rubie, D.C. et al. (2011), Heterogeneous accretion, composition and core-mantle differentiation of the Earth, *Earth Planet. Sci. Lett.*, *301*, 31–42.
- Rudge, J. F., T. Kleine, and B. Bourdon (2010), Broad bounds on Earth's accretion and core formation constrained by geochemical models, *Nature Geosci.*, *3*, 439–443.
- Samuel, H. (2012), A re-evaluation of metal diapir breakup and equilibration in terrestrial magma oceans, *Earth Planet. Sci. Lett.*, *313*, 105–114.
- Sasaki, T. and Y. Abe (2007), Rayleigh-Taylor instability after giant impacts: Imperfect equilibration of the Hf-W system and its effect on the core formation age, *Earth Planet. Space*, *59*, 1035–1045.
- Schersten, A., T. Elliott, C. Hawkesworth, S. Russell, and J. Masarik (2006), Hf-W evidence for rapid differentiation of iron meteorite parent bodies, *Earth Planet. Sci. Lett.*, *241*, 530–542.
- Schönbächler, M., R. W. Carlson, M. F. Horan, T. D. Mock, and E. H. Hauri (2010), Heterogeneous accretion and the moderately volatile element budget of Earth, *Science*, *328*, 884–886.
- Schönberg, R., B. S. Kamber, K. D. Collerson, and O. Eugster (2002), New W-isotope evidence for rapid terrestrial accretion and very early core formation. *Geochim. Cosmochim. Acta.*, *66*, 3151–3160.
- Siebert, J., J. Badro, D. Antonangeli, and F. J. Ryerson (2013), Terrestrial accretion under oxidizing conditions, *Science*, *339*, 1194–1197.
- Solomatov, V. S. (2000), Fluid dynamics of a terrestrial magma ocean, in Canup, R. M. and K. Righter, Eds., *Origin of the Earth and Moon*, Univ. Arizona Press, pp. 323–338.
- Sramek, O., Y. Ricard, and F. Dubuffet (2010), A multiphase model of core formation, *Geophys. J. Int.*, *181*, 198–220.
- Stevenson, D. J. (1990), Fluid dynamics of core formation, in Newsom, H. E. and J. E. Jones, Eds., *Origin of the Earth*, Oxford Univ. Press, pp. 231–249.
- Tang, H. and N. Dauphas (2012), Abundance, distribution and origin of Fe-60 in the solar protoplanetary disk, *Earth Planet. Sci. Lett.*, *359*, 248–263.
- Tonks, W. B. and H. J. Melosh (1993), Magma ocean formation due to giant impacts, *J. Geophys. Res.*, *98*, 5319–5333.
- Touboul, M., I. S. Puchtel, and R. J. Walker (2012), W-182 evidence for long-term preservation of early mantle differentiation products, *Science*, *335*, 1065–1069.
- Touboul M., T. Kleine, B. Bourdon, Van Orman J. A., C. Maden, and J. Zipfel (2009), Hf-W thermochronometry II: Accretion and thermal history of the acapulcoite-lodranite parent body, *Earth Planet. Sci. Lett.*, *284*, 168–178.
- Touboul, M., T. Kleine, B. Bourdon, H. Palme, and R. Wieler (2007), Late formation and prolonged differentiation of the Moon inferred from W isotopes in lunar metals, *Nature*, *450*, 1206–1209.
- Touboul, M., J. Liu, J. O'Neil, I. S. Puchtel and R. J. Walker (2014), New insights into the Hadean mantle revealed by ¹⁸²W and highly siderophile element abundances of supracrustal rocks from the Nuvvuagittuq Greenstone Belt, Quebec, *Canada. Chem. Geol.*, *383*, 63–75.
- Touboul, M., P. Sprung, S. A. Aciego, B. Bourdon, and T. Kleine (2015b), *Hf-W chronology of the eucrite parent body*, *Geochim. Cosmochim. Acta*, *156*, 106–121.
- Touboul, M., I. Puchtel, and R. J. Walker (2015), Tungsten isotopic evidence for disproportional late accretion to the Earth and Moon, *Nature*, *520*, 530–533.
- Tsuno, K., D. J. Frost, D. C. Rubie (2013), Simultaneous partitioning of silicon and oxygen into the Earth's core during early Earth differentiation, *Geophys. Res. Lett.*, *40*, 66–71.
- Tucker, J.M. and S. Mukhopadhyay (2014), Evidence for multiple magma ocean outgassing and atmospheric loss episodes from mantle noble gases, *Earth Planet. Sci. Lett.*, *393*, 254–265.

- Wade, J. and B. J. Wood (2005), Core formation and the oxidation state of the Earth, *Earth Planet. Sci. Lett.*, 236, 78–95.
- Walker, R. J. (2014), Siderophile element constraints on the origin of the Moon, *Phil. Trans. R. Soc. Lond., A*, 372, 20130258.
- Walsh, K. J., A. Morbidelli, S. N. Raymond, D. P. O'Brien, and A. M. Mandell (2011), A low mass for Mars from Jupiter's early gas-driven migration, *Nature*, 475, 206–209.
- Wang, Z. and H. Becker (2013), Ratios of S, Se and Te in the silicate Earth require a volatile-rich late veneer, *Nature*, 499, 328–331.
- Willbold, M., T. Elliott, and S. Moorbath (2011), The tungsten isotopic composition of the Earth's mantle before the terminal bombardment, *Nature*, 477, 195–197.
- Wood, B. J. and A.N. Halliday (2010), The lead isotopic age of the Earth can be explained by core formation alone. *Nature*, 465, 767–771.
- Wood, B. J., J. Wade, and M. R. Kilburn (2008), Core formation and the oxidation state of the Earth: additional constraints from Nb, V and Cr partitioning. *Geochim. Cosmochim. Acta.*, 72, 1415–1426.
- Wood, B. J., A. N. Halliday, and M. Rehkamper (2010), Volatile accretion history of the Earth, *Nature*, 457, E6–E7.
- Yang, J. and J. I. Goldstein (2006), Metallographic cooling rates of the IIIAB iron meteorites, *Geochim. Cosmochim. Acta.*, 70, 3197–3215.
- Yang, J., J. I. Goldstein, and E. R. D. Scott (2007), Iron meteorite evidence for early formation and catastrophic disruption of protoplanets, *Nature*, 446, 888–891.
- Yin Q. Z., S. B. Jacobsen, K. Yamashita, J. Blichert-Toft, P. Telouk, and F. Albarede (2002), A short timescale for terrestrial planet formation from Hf-W chronometry of meteorites. *Nature*, 418, 949–952.
- Yoshino, T., M. J. Walter, and T. Katsura (2003), Core formation in planetesimals triggered by permeable flow, *Nature*, 422, 154–157.
- Zahnle, K., N. Arndt, C. S. Cockell, A. Halliday, E. Nisbet, F. Selsis, and N. H. Sleep (2007), Emergence of a habitable planet, *Space Sci. Rev.*, 129, 35–78.
- Zhang, J. J., N. Dauphas, A. M. Davis, I. Leya, and A. Fedkin (2012), The proto-Earth as a significant source of lunar material, *Nature Geosci.*, 5, 251–255.